

Research of Computed Tomography Inversion Algorithm for Coal Face Based on Ground Penetrating Radar

YANG Feng

School of Mechanical Electronic & Information Engineering,
China University of Mining and Technology (Beijing)
Beijing, China

DU Cui¹, PENG Meng², FENG Zequan¹, SUN Yangyang¹, LI Enlai²

1 School of Mechanical Electronic & Information Engineering,
2 College of Geoscience and Surveying Engineering,
China University of Mining and Technology (Beijing)
Beijing, China

Abstract—Currently, mine safety is the focal point in mining activity. As a new and advanced approach for geophysical prospecting, the ground penetrating radar (GPR) is used in the mine disaster detection. Aiming to solve the restriction of low resolution and limited depth of the GPR in the deep coal seam detection, the computed tomography (CT) technology is employed for deep disaster detection in this paper. A large number of coal seam digital simulation model, including different internal diseases, are established, and the simulation data are processed by using the Least Square QR-factorization (LSQR) inversion algorithm, which has the good performance in saving computational time and memory space. Additionally, the influences of iteration precision and grid size on the effect of inversion are analyzed. The inversion results show good agreements with simulation model feature configurations, and the diseases objects can be detected.

Keywords- GPR; CT inversion; sparse matrix; coal face; disaster sources

I. INTRODUCTION

Ground penetrating radar (GPR), as a noninvasive technique to identify and classify subsurface features, has received much attention in wide variety of application fields, such as coal mine, subgrade of highway and large dam projects. Compared with electric method, GPR's advantage lies in the direct identification for underground objective without complicated theoretical inference (Peng et al. 2010, Chen et al. 2010). It has become one of the most important means in the field of shallow geophysical prospecting.

Currently, reflection technology is commonly used in GPR projects. It sends high-frequency electromagnetic waves and makes use of the difference of the electrical property of underground medium to analyze and deduce the structure and character of the medium, based on kinematics and dynamics character of the wave, such as swing, wave form and frequency (Yang et al. 2002). However, due to poor reflection signal, the detection range is confined to within 100 meters below the surface. Consequently, the GPR image resolution is not high enough in deep coal seam detection. This research implements computed tomography (CT) technology into GPR. It makes use of transmission wave whose energy attenuation is much lower. Hence image resolution can be greatly improved and mine disaster sources detected correctly.

The complexity of coal mine underground environment, coupled with limitation of detection means, lead to lack of data, so the coefficient matrix is usually large and sparse. As a result, the inversion equations are both ill-conditioned and have multiple solutions. Another challenge in CT is the uneven distribution and shortage coverage of detection rays. It is difficult to avoid local distortion when imaging. The present paper uses least square QR-factorization (LSQR) algorithm to solve inversion equations. To simulate coal mine environment, a series of coal seam digital model are established, designed with different disaster sources. Considering inversion efficiency, relative influencing factors are tested.

The organization of this paper is as follows. Section 2 presents a short description of the principle of CT used in GPR projects. Section 3 focuses on the inversion algorithm that is developed to boost the ability for ill-conditioned equations. Section 4 presents experimental results and the influence of iteration precision as well as grid size on the effect of inversion is analyzed respectively. Finally, section 5 contains the concluding remarks.

II. THEORY OF CT FOR GPR

A. GPR Detection Method with CT Employed

Fig.1 is the schematic drawing of CT detection. The transmitting antenna is arranged at one side of the selected coal face profile and receiving antenna the opposite side. Both sides are divided into equal distance. Each segment's midpoint is a measuring point. When GPR is used for CT detection, transmitting antenna is fixed at t_1 , and receiving antenna moves from r_1 to r_n ; with transmitting antenna fixed at t_2 , receiving antenna still moves from r_1 to r_n ; for each transmitting point, receiving antenna moves n times.

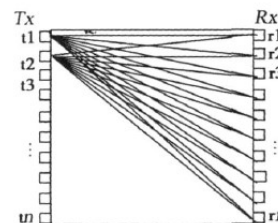


Figure1. Schematic diagram of CT detection using GPR

B. Velocity Tomography Inversion

CT for GPR is divided into two main classes: velocity tomography inversion and attenuation tomography inversion. The former images wave velocity of the profile medium according to first arrive time of receiving waveform; the latter images decay coefficient of the profile medium based on amplitude or frequency information of receiving waveform. This research is focused on velocity tomography inversion. The geological structure of the detected profile can be gained based on the relationship between medium wave velocity and material composition.

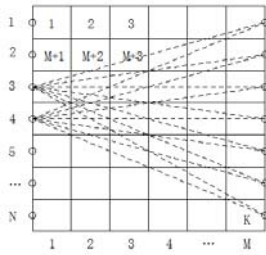


Figure2. Discretized model of detected profile

According to the detection project, the profile is discretized into a rectangle model of M columns and N rows. There are K (K=M×N) grids in all. Fig.2 shows the discretization result.

It is assumed that the electromagnetic wave travels in straight lines in medium of small velocity difference (less than 10% ~ 15%). The travel time can be expressed by linear integral of velocity's reciprocal (namely slowness).

The slowness of the kth grid's medium is set as an average value x_k ,

$$t_i^j = \sum_{k=1}^{M \times N} L_{ij}^k x_k$$

where t_i^j represents the travel time of the ray transmitted by the ith transmitting point and received by the jth receiving point, L_{ij} indicates the length of this ray in the kth grid, x_k is the slowness of the kth grid.

For a certain i, j is from 1 to N, and then we can get the following equations,

$$\begin{cases} t_i^1 = \sum_{k=1}^{M \times N} L_{i1}^k x_k \\ t_i^2 = \sum_{k=1}^{M \times N} L_{i2}^k x_k \\ t_i^j = \sum_{k=1}^{M \times N} L_{ij}^k x_k \\ t_i^N = \sum_{k=1}^{M \times N} L_{iN}^k x_k \end{cases}$$

The equations can be written in the form $T_i=L_iX$. T_i is a vector of travel times of rays transmitted at ith point, which are detected data. L_i is a matrix consisted by the length in each grid of these rays, which can be calculated out. X is a vector of slowness values of each grid. It is X that we desire to get through inversion.

The i is also ranged from 1 to N. Eventually we get $N \times N$ equations, which can be expressed as $T=LX$. The matrix will normally be large and sparse. Hence the essence of CT inversion is to find an appropriate algorithm for solve this equations.

III. CT INVERSION ALGORITHM

A. Coefficient Matrix

According to the principle of velocity tomography, coefficient matrix consists of the length of each ray in each grid. A general method is to traverse all the grids within the model for all rays. However, it costs lots of time and memory. In order to overcome the shortcoming, this research presents efforts to overcome the constraint and limitations by tracking the trend of the ray so that only calculating grids rays go through.

For each ray, the slope can be got according to position of transmitting and receiving point. The calculating begins at the grid that transmitting point lies in. The next grid that the ray goes through can be obtained from slope and right intercept of the last one.

B. LSQR Algorithm

Based on the front analysis, the primary goal is to solve a large and sparse equations $T=LX$. For inversion algorithm design, it is important to consider non-uniqueness of solutions.

LSQR finds a solution to the following problem:

Linear least squares: minimize $\|Ax-b\|_2$

where A is a matrix with m rows and n columns, b is an m-vector. A is coefficient matrix and b is detected data of time.

LSQR uses an algorithm of Golub and Kahan to reduce A to lower diagonal form. It is assumed that $U_k=[u_1, \dots, u_k]$ and $V_k=[v_1, \dots, v_k]$ are orthogonal matrices and B_k are down double diagonally matrix of $(k+1) \times k$ as following:

$$B_k = \begin{bmatrix} \alpha_1 & \dots & \dots \\ \beta_2 \alpha_2 & \dots & \dots \\ \dots & \dots & \alpha_k \\ \dots & \dots & \beta_{k+1} \end{bmatrix}$$

Using the following iterative method can make matrix A double diagonal decomposed:

$$\begin{cases} \beta_1 u_1 = b, \alpha_1 v_1 = A^T u_1 \\ \beta_{i+1} = A v_i - \alpha_i u_i \\ \alpha_{i+1} v_{i+1} = A^T \beta_{i+1} v_i \end{cases} \quad i=1, 2, \dots$$

Setting $\|u_i\| \equiv \|v_i\| \equiv 1$, the expression can be rewritten like:

$$\begin{cases} U_{k+1}(\beta_1 e_1) = b \\ AV_k = U_{k+1}B_k \\ A^T U_{k+1} = V_k B_k^T + \alpha_{k+1} v_{k+1} e_{k+1}^T \end{cases}$$

where e_{k+1}^T represents the $k+1$ th row of a n level unit matrix. Further, we set

$$x_k = V_k y_k, r_k = b - Ax_k, t_{k+1} = \beta_1 e_1 - B_k y_k$$

so we can ensure

$$\begin{aligned} r_k &= b - Ax_k = U_{k+1}(\beta_1 e_1) - AV_k y_k \\ &= U_{k+1}(\beta_1 e_1) - U_{k+1}B_k y_k = U_{k+1}t_{k+1} \end{aligned}$$

The iteration stops when requirement of the given precision satisfied.

IV. RESULTS OF SIMULATION EXPERIMENTS

A. Inversion Affection of Simulation Experiment

A model with 10 rows and 20 columns is designed, including a disease area. Each grid has the same size. There are 10 transmitting points and 10 receiving points located at the midpoint of grid line.

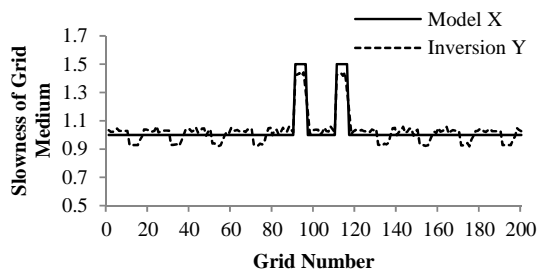


Figure3. Comparison of model and inversion results

The inversion equations $AX=B$ is established. B is calculated from A and X . Then $AY=B$ is solved through LSQR. The inversion affection can be checked by comparing X and Y .

Fig.3 shows that inversion results shows quite agreement with the designed model. The error is within 1%. The location of disease area is found and the medium of this area can be determined correctly.

B. Influence of Inversion Precision

A model with 10 rows and 10 columns is designed. There are 10 transmitting points and 10 receiving points located at the midpoint of grid line.

Experiments are carried out with four different requirements of inversion precision. In Fig.4, we can see that the normal trend is that the higher precision, the better inversion affection. But no clear difference exists among $1.00E+05$, $1.00E+06$ and $1.00E+07$.

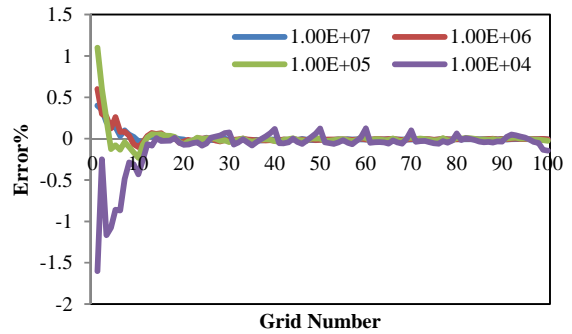


Figure4. Errors in different requirements of inversion precision

In Fig.5, it is clear to see that both iterations and iteration time increase in linear as precision increases. Precision is a critical factor in an algorithm especially dealing with large amounts of data. To design an efficient algorithm, it is important to choose appropriate magnitudes while considering inversion requirement and inversion cost.

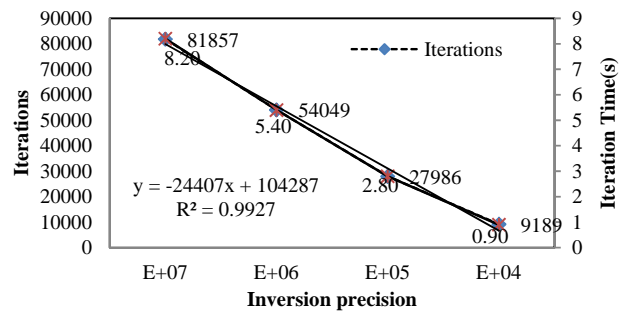


Figure5. Iterations and iteration time of different requirements of inversion precision

C. Influence of Grid Size

A model with 10 rows and 40 columns is designed, including 7 disease areas. Each grid has the same size. There are 10 transmitting points and 10 receiving points located at the midpoint of grid line. All the disease areas are square ones. The line lengths are respectively 1~7 integral multiple of the grid's.

Fig.6 illustrates that grid size is related closely with effect of inversion. The smaller proportion of the ratio of grid size to disease area length basically corresponds to the better effect of inversion. When ratio reaches $1/4$, the best effect is achieved.

V. CONCLUSIONS

In this paper, computed tomography technology is employed in GPR detection.

LSQR is an effective algorithm for solving large sparse inversion equations. The simulation experimental results show that GPR can achieve high detection accuracy with CT technology. Considering inversion cost of time and computer memory, precision of $1.00E+05$ is appropriate. The ratio of grid size to disease area length is an important

inversion parameter. In the first inversion, the size of disaster area is detected. Setting ratio of grid size to disease area length as 1/4 in the next inversion could contribute better inversion effect.

Future directions are to further improve this method to capture accurate edges of coal mine disaster sources then get its more precise position.

ACKNOWLEDGMENT

This study was supported by Special Development of National Key Scientific Equipment (2012YQ030126) and two "Twelfth Five-Year" Plan key projects supported by National Science and Technology" (2011BAK06B01-06 and 2011BAD04B05).

REFERENCES

[1] Y.C.Chen,B.X.Xiao.Situation and Development of Ground Penetrating Radar. Chinese Journal of Engineering Geophysics,2005(2),149-155.

[2] F.Yang, S.P.Peng. Detecting Theory and Method Research of Ground Penetrating Radar. Beijing:Science Publishing Company,2010.

[3] D.J.Danels(2004). Ground Penetrating Radar. 2nd ed.London: The Institute of Electrical Engineers.

[4] W.Yang, S.X.Liu, Y.Q.Feng. Research of Cross-hole tomography LSQR Algrithem. Geophysical and Geochemical Exploration, 2008(2):199-202.

[5] J.Yang.(2011) "The Research of Detection of the Underground Pipe's Diameter Based on GPR" Beijing: China University of Mining and Technology(Beijing),pp.31-33.

[6] D.Zhang et al. Fast Solving of LSQR Algrithem in Seismic Tomography. Geophysical and Geochemical Exploration Computing. 2011(6): 632-635+574.

[7] Meles G A, Kruk J V d, Stewart A, etal. A New Vector Waveform Inversion Algorithm for Simultaneous Updating of Conductivity and Permittivity Parameters From Combination Crosshole/Borehole-to-Surface GPR Data. IEEE Transactions on Geoscience and Remote Sensing, 2010, 48(9):3391-3407.

[8] Belina F, Irving J, Ernst J, etal. Analysis of an Iterative Deconvolution Approach for Estimating the Source Wavelet During Waveform Inversion of Crosshole Georadar Data. Journal of Applied Geophysics, 2012(78), 20-30.

[9] Carlsten S, Johansson S, Worman A. Radar Techniques for Indicating Internal Erosion in Embankment Dams. J. Appl. Geophys., 1995,33(1-3):143-156.

[10] Holliger K, Bergmann T. Numerical Modeling of Borehole Georadar Data.Geophysics, 2002, 67(4):1249-1257.

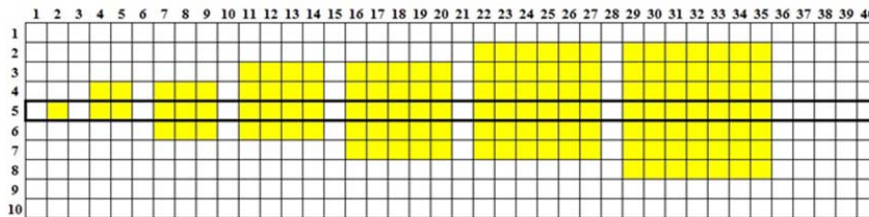


Figure6. Profile model for grid size experiments

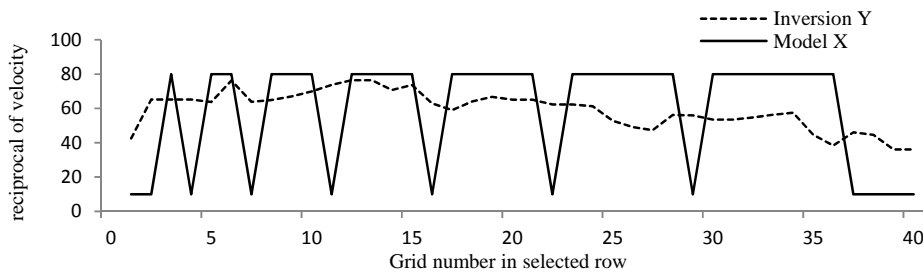


Figure7. Inversion results of the 5th row